Environ. Sci. Technol. **2008,** *42,* 1102–1108

Virus Transport during Infiltration of a Wetting Front into Initially Unsaturated Sand Columns

ANDREW B. KENST,[†]
EDMUND PERFECT,*[,†]
STEVEN W. WILHELM,[‡] JIE ZHUANG,[†]
JOHN F. MCCARTHY,[†] AND
LARRY D. MCKAY[†]

Departments of Earth and Planetary Sciences and Microbiology, University of Tennessee, Knoxville, Tennessee 37996

Received May 23, 2007. Revised manuscript received September 14, 2007. Accepted November 27, 2007.

We investigated the effect of different flow conditions on the transport of bacteriophage ϕX174 in Memphis aquifer sand. Virus transport associated with a wetting front moving into an initially unsaturated horizontal sand column was experimentally compared with that observed under steady-state saturated vertical flow. Results obtained by sectioning the sand columns show that total (retained and free) resident virus concentrations decreased approximately exponentially with the travel distance. The rate of decline was similar under both transient unsaturated flow and steady-state saturated flow conditions. Total resident virus concentrations near the inlet were an order of magnitude greater than the virus concentration of the influent solution in both experiments, indicating continuous virus sorption during flow through this zone. Virus retardation was quantified using the ratio of the centroids of the relative saturation and virus concentration versus relative distance functions. The mean retardation factors were 6.43 (coefficient of variation, CV = 14.4%) and 8.22 (CV = 8.22%) for the transient unsaturated and steady-state saturated flow experiments, respectively. A *t* test indicated no significant difference between these values at $P < 0.05$. Air–water and air–water−solid interfaces are thought to enhance virus inactivation and sorption to solid particles. The similar retardation factors obtained may be attributable to the reduced presence of these interfaces in the two flow systems investigated as compared to steady-state unsaturated flow experiments in which these interfaces occur throughout the entire column.

Introduction

More than 100 million people in the United States depend on underground sources for their potable water supply (*1*). Annually, ~50% of America's disease outbreaks are caused by contaminated groundwater (*2*). While strict guidelines for treating surface waters for microbial contaminants exist, regulations for controlling systems that use groundwater are less stringent (*3*). Aquifers are subject to microbial contamination, both viral and bacterial, from a variety of sources, such as land application of human waste, broken sewer lines, and animal manure disposal (*4*). Septic-tank effluent is probably the greatest source of pathogenic viruses found in groundwater (*5*). Viruses are of greater concern than bacteria and protozoa because they are much smaller in size and might not be filtered out of soil–water solutions as easily as larger microorganisms (*6*).

Predicting groundwater vulnerability to viral contamination and modeling transport of these organisms is presently limited by an incomplete understanding of the factors that influence virus fate and transport. The ability of a porous medium to filter, or disinfect, biologically contaminated water depends on several factors thought to influence virus inactivation and/or adsorption to solid surfaces during flow (*6*). These factors include soil-water pH, soil-solution ionic strength, metal oxides coating soil grains, and the mass-fraction of organic carbon present. Properties of the virus protein coat, such as surface charge, also affect their movement through soils and aquifer material.

In the vadose zone, water content and flow conditions play important roles in virus transport. Experimental and theoretical studies (*7, 8*) indicate an increase in interfacial area with decreasing wetting phase saturation. Air–water (AW) and/or air–water−solid (AWS) interfaces are thought to contribute to an increase in virus inactivation, while decreasing saturation increases the likelihood of viruses attaching to solid particles (*9–11*)

The majority of previous virus transport studies have been laboratory column experiments conducted under steady-state saturated flow conditions. To date, only a few studies have investigated virus transport under partially saturated conditions, and most of these were for steady-state flow (*9–16*). Under such conditions, variable saturation occurs throughout the entire transport domain, water films tend to be thinner and more tortuous, and many AW/AWS interfaces are present.

Steady-state unsaturated flow rarely occurs in nature. Most flow in the vadose zone occurs under transient conditions, in which a zone of near saturation forms behind the wetting front as water advances into previously unsaturated soil (the so-called transmission zone). This is the case with septic tank effluent (*17*). Under such conditions, transport takes place through a near-saturated transmission zone and AW/AWS interfaces are greatly reduced as compared to steady-state unsaturated flow, suggesting reduced virus inactivation and sorption.

The overall goal of this research was to determine the effect of transient unsaturated flow conditions on the transport of viruses in a porous medium. Van Cuyk et al. (*17*) studied virus removal during long-term episodic flows through variably saturated granular media based on effluent concentrations. To our knowledge, however, no one has previously investigated resident virus concentrations during the infiltration of a wetting front. We hypothesized that, because of reduced AWS interfaces, virus retardation during transient unsaturated flow would be similar to virus retardation during steady-state saturated flow.

Materials and Methods

Aquifer Material Characterization. The Memphis aquifer, composed of unconsolidated sand and overlain by loess, supplies much of the water used in west Tennessee. The sand dates to the early to mid-Tertiary period. The aquifer outcrops in eastern Shelby County, Tennessee where mi-

* Corresponding author phone: (865) 974-6017; fax: (865) 974-2368; e-mail: eperfect@utk.edu.
[†] Department of Earth and Planetary Sciences, University of Tennessee.
[‡] Department of Microbiology, University of Tennessee.

10.1021/es071213s CCC: $40.75
Published on Web 01/17/2008

TABLE 1. Virus Influent Concentrations, C_o, Mass Balance Information, and Estimated Retardation Coefficients, R, for the Transient Unsaturated and Steady-State Saturated Flow Experiments

	transient unsaturated flow			steady-state saturated flow		
replication	C_0 (pfu mL^{-1})	recovery (%)	R	C_0 (pfu mL^{-1})	recovery (%)	R
1	1.07×10^6	11.5	6.20	4.35×10^6	56.9	11.9
2	1.61×10^6	60.7	6.33	4.64×10^6	19.2	5.80
3	6.08×10^6	52.4	6.77	5.17×10^6	20.2	6.96
average	2.92×10^6	41.5	6.43	4.72×10^6	32.1	8.22
CV (%)	9.41	63.4	14.4	8.73	66.9	38.3

crobiological contamination is becoming a concern because of the large number of septic systems in the aquifer recharge zone.

Composite samples of Memphis aquifer sand were collected in rotasonic cores over a depth interval of 32.0−33.8 m from a field site at Shelby Farms, Shelby County, TN. The median particle size was ∼300 μm. The silt and clay fractions comprised <1.4% of the sample. The remainder was very fine to medium sand. The mean particle density (ρ_s) determined using the pycnometer method (*18*) was 2.59 (±0.04) Mg/m^3.

A tension table, similar to the sand tank described by Kutílek and Nielsen (*19*), was used to measure the main drying-branch of the water retention curve. Memphis aquifer sand was packed in metal rings to a bulk density (ρ_b) of ∼1.6 Mg m^{-3}, and saturated from below overnight. Desorption measurements were performed in triplicate over the tension range 0 to 0.7 m. The data were averaged and graphically parameterized using the Brooks and Corey model (*19*). The resulting model parameters were: $\theta_s = 0.45$,$\theta_r = 0.09$, $h_a =$ 0.316 m, and $\beta = 5.85$, where θ_s is the volumetric water content at saturation, θ_r is the residual volumetric water content, h_a is the air entry head, and β is the pore-size distribution index. These values indicate a medium sand with a narrow pore size distribution.

The saturated hydraulic conductivity (K_{sat}) was measured using vertical, saturated columns with a constant head technique adapted from methods described by Reynolds et al. (*20*). The columns were packed to approximately the same density as the rings used for the water retention measurements. The geometric average K_{sat} for three replicates of Memphis Aquifer sand was 8.34×10^{-5} m s^{-1} with a standard deviation factor of 1.11.

Chemical characterization of the Memphis aquifer sand was performed by the Agricultural Extension Service of the University of Tennessee Institute of Agriculture. The Mehlich 1 extraction method was used to test for elements which could influence virus transport (*21*). The resulting P, K, Ca, Mg, and Fe contents were 1.8, 7.3, 42.1, 11.9, and 8.7 mg kg^{-1}, respectively. On the basis of the Walkley and Black method, which measures the amount of oxidizable organic carbon in soil (*22*), the organic matter content was 0.4%. The soil–water pH was 5.7 as determined with an electrometer in a deionized water slurry (*23*).

Bacteriophage Assay Procedures. Bacteriophages are often used as analogs for pathogenic human viruses because they possess many of the same physical and chemical characteristics of such pathogens, but are safer to work with. Bacteriophage ϕX174 has been used to model a variety of enteric viruses including caliciviruses such as Norwalk and Norwalk-like viruses (*24, 25*). It was used in this study because it is easy to culture and assay, is noninfectious to humans, and is well documented in previous column studies. Bacteriophage ϕX174 (ATCC 13706-B1), and its host *Escherichia coli* (ATCC 13706), are currently available from the American Type Culture Collection (ATCC). It is a hydrophilic, single-stranded DNA phage ranging in diameter from 25 to 27 nm, and has an isoelectric point (pH_{IEP}) of 6.6 (*26*).

Methods regarding the culture and handling of ϕX174 and its host bacteria were based on information provided by ATCC. All experiments were conducted at room temperature (∼20 °C), and all virus samplings were performed in duplicate. Viruses were enumerated using the agar-layer assay technique described by Adams (*27*). In brief, a solution containing viruses is serially diluted and added to nutrient agar that contains a lawn of host bacteria. As the viruses replicate, clearings in the lawn known as plaques appear indicating dead bacteria. Each plaque forms from a single virus particle referred to as a plaque forming unit (pfu). The plaques are then counted and calculations made to determine the number of pfu's in the original solution. The error associated with this procedure is ±20% (*10*). Mass recovery was calculated by dividing the total number of viruses eluted from a column by the total number of viruses input to that column.

Transient Unsaturated Flow Experiments. A 0.2 m long horizontal column with an inside diameter of 20.5 mm constructed of clear polyvinyl chloride (PVC) was used for the three replicate transient unsaturated flow experiments. The column was scored in 10 mm increments using a pipe cutter to facilitate rapid segmentation of the column at the end of the experiment. The empty column was weighed, then packed with air-dry Memphis Aquifer sand using a standard tap and fill method (*28*). The mean ρ_b of the columns used in these experiments was 1.61 Mg m^{-3} (±0.003). Both ends of the packed column were equipped with a PVC fitting that contained a sintered stainless steel plate with an average pore size of 100 μm and a rubber gasket to seal the tube and steel plate. This allowed a phosphate buffer saline (PBS) solution containing viruses (∼1×10^6 pfu mL^{-1}, Table 1) to enter the column and air to exit at the other end as the solution infiltrated. The PBS is composed of Na_2HPO_4 (20 mM), NaCl (100 mM), and KCl (3 mM), has an ionic strength of 0.163 M and pH of 7.5, and is commonly used in virus transport experiments (*29*). Teflon tubing was used throughout the apparatus, except for the influent fitting which was PVC. The column materials were tested for virus interaction by slowly pouring 300 mL of PBS containing ∼1×10^6 pfu mL^{-1} of virus through an empty column and collecting the effluent. The concentration of ϕX174 in the effluent showed no measurable change from the influent concentration, thus indicating minimal interaction between the viruses and the materials used in the apparatus.

The PBS and virus solution were introduced to the packed column under zero pressure head from a Marriotte bottle equipped with a bubbling tube (Figure 1). Movement of the wetting front into the column by capillarity caused a diminution of the matric potential gradient over time ensuring variable flow rates. The wetting front was allowed to infiltrate a distance of ∼150 mm before the supply was stopped. This left at least four air-dry column segments to act as controls. At the end of the experiment the column was detached from the Marriotte bottle and sealed at the influent end to minimize PBS and virus redistribution within the column.

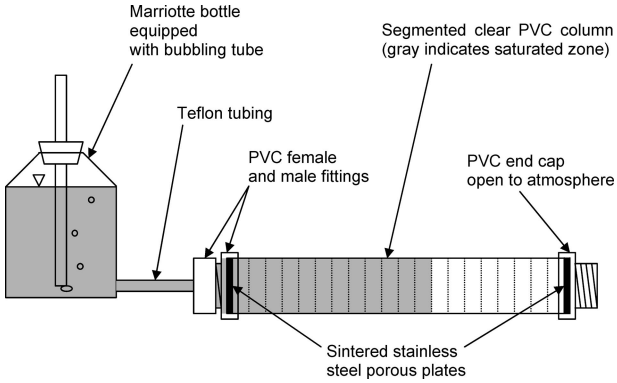

FIGURE 1. Column design for the transient unsaturated flow experiments.

The sealed column was immediately segmented using a pipe cutter, and each segment was weighed to determine the gravimetric water content, w. Sand from each segment was then washed into 15 mL polypropylene centrifuge tubes with beef extract solution (BEX). BEX is commonly used to desorb viruses from soil (*30, 31*). Each sample was shaken by hand for five seconds to mix the BEX, sand, and PBS. The samples were then allowed to equilibrate for two hours at room temperature, after which they were serially diluted in PBS and added to borosilicate glass tubes containing 0.5 mL of high concentration *E. coli* stock and 4 mL of 0.6% top agar maintained at 40 °C. The glass tube was vortexed briefly and poured into a Petri dish warmed to 37 °C and containing 2.3% bottom agar prepared according to ATCC instructions. The plate was rocked to spread the 0.6% top agar, allowed to cool, then placed in an incubator. Plaques became visible after ~5 h, at which point they were counted. Multiplying the number of plaques on a plate by the dilution factor yields the concentration of virus in the sampled volume of liquid. The number of viruses in the sampled PBS solution relative to the number of viruses initially input to each tube was determined by multiplying the number of pfu's on a plate by the volume of liquid in the tube.

The relative water content or relative saturation, $S_r \equiv \theta/\theta_s$ (where θ is the volumetric water content) of each segment was calculated from the measured w, ρ_b and ρ_s values using the expression $S_r = w/\rho_l/\rho_b - \rho_l/\rho_s$, with ρ_l assumed to be 1 Mg m^{-3}. The resident virus concentration, C (pfu m^{-3}), was determined from the total (free and retained) number of viruses eluted from each column segment (pfu segment^{-1}) divided by the volume of each column segment (m^3 segment^{-1}). The C is related to the virus concentration in the pore water, C_w (pfu mL^{-1}), and the sorbed virus concentration, C_s (pfu g^{-1}), by

$$C = \theta C_w + \rho_b C_s \tag{1}$$

The relative virus concentration was calculated as $C_r \equiv C/C_o$ (where C_o is the virus concentration of the input solution (pfu m^{-3})). These quantities were then expressed as functions of the relative transport distance ($x \equiv d/d_{\max\ water}$, where d is distance from the inflow end (m) and $d_{\max\ water}$ is the maximum distance the wetting front moved (m), as indicated by the occurrence of the first dry column segment).

The effective virus retardation coefficient, R, was estimated from the ratio of the centroids for the relative water content and relative virus concentration functions. This approach was originally proposed by Smiles et al. (*32*) for the hydrodynamic dispersion of an inert solute during convective replacement of resident pore water by an invading solution. It was subsequently extended to the reactive transport of cations and anions in unsaturated soils (*33–35*), and has recently been applied to the sorption of hydrophilic organic compounds (*36–38*). Here, we employ it to quantify virus retardation during infiltration of a virus-spiked solution into an initially dry porous medium (i.e., zero resident pore water).

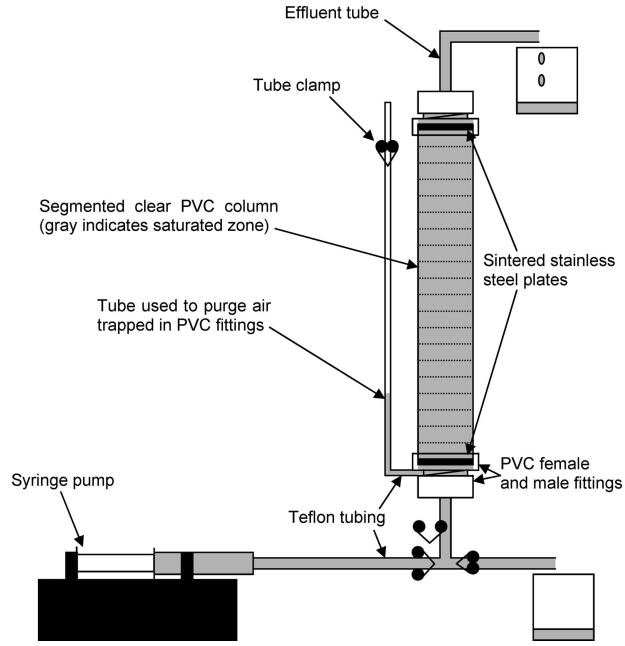

FIGURE 2. Column design for the steady-state saturated flow experiments.

The integral expressions defining the centroid of each function are given below:

$$\int_0^{S_{max}} x\,dS_r = \int_0^{\lambda_w} S_r\,dx \tag{2a}$$

$$\int_0^{C_{max}} x\,dC_r = \int_0^{\lambda_v} C_r\,dx \tag{2b}$$

where S_{max} is the maximum saturation as $x \rightarrow 0$, λ_w is the centroid of the relative water content function, C_{max} is the maximum relative virus concentration as $x \rightarrow 0$ and λ_v is the centroid of the relative virus concentration function. The areas under the curves were computed by numerical integration, and the centroids determined by finding the values of $d/d_{\max\ water}$ that divided each area into two equal halves. The retardation coefficient was then calculated using the following expression (*33*)

$$R = \frac{\lambda_w}{\lambda_v} \tag{3}$$

Steady-State Saturated Flow Experiments. Three replicate, steady-state saturated flow column experiments were conducted for comparison with the transient unsaturated flow experiments. A 0.2 m segmented PVC column was packed with air-dry Memphis aquifer sand to the same ρ_b as the transient unsaturated flow columns. The column was then positioned vertically and saturated from the bottom-up overnight with autoclaved, deaired PBS to expel any entrapped air. Next, the bottom of the column was attached to a Harvard Apparatus programmable PHD 2000 nonpulsing syringe pump, which injected PBS and virus solution (~1×10^6 pfu mL^{-1}, Table 1) at a constant flux of 0.21 mm s^{-1} (Figure 2). The duration of pumping was 12 min, which was approximately the same as the duration of the unsaturated transient flow experiments. At the end of the experiment, the column was segmented and sampled for viruses as described for the transient unsaturated flow experiments.

Relative saturation and relative virus concentration were calculated for each column segment and expressed as functions of $d/d_{\max\ water}$. Because the columns were fully saturated, $\theta/\theta_s = 1$ for all of the segments. Therefore, $d_{\max\ water}$ was calculated as the maximum distance the influent solution traveled into the column based on the porosity and volume of water input to the column over the duration of the experiment. It follows that $\lambda_w = d_{\max\ water}/2$. Equation (*3*) was then used to calculate R with λ_ν determined using the same method as described previously.

Batch Experiments. Batch experiments were conducted to determine the partitioning of bacteriophage ϕX174 when exposed to Memphis Aquifer sand. All the batch experiments were performed using PBS solution containing approximately 1×10^4, 1×10^5, 1×10^6, and 1×10^7 pfu mL^{-1} concentrations. This range of inputs was chosen because the input virus concentration used for the column experiments was $\sim 1 \times 10^6$ pfu mL^{-1}. Conditions for the batch experiments were designed to be as similar as possible to those for the column flow experiments regarding time, temperature, and sampling protocol. Three replicate batch experiments were performed.

Five grams of Memphis Aquifer sand were added to sterile 15 mL polypropylene centrifuge tubes, each containing 4 mL of PBS with viruses at a concentration equal to one of the four concentrations given above. Adding sand to the PBS ensured complete saturation of the sand. The samples were allowed to equilibrate for 20 min, and then the liquid supernatant was sampled. The sampled supernatant was serially diluted in PBS and assayed as described for the transient unsaturated flow experiments. Next, the number of viruses sorbed to solids was calculated by difference, assuming there was no loss of viruses due to inactivation. This gave virus partitioning between the liquid and solid phases of the soil and PBS solution under saturated, zero-flux conditions.

Results

Transient Unsaturated Flow Experiments. The relative saturation, θ/θ_s, and relative virus concentration, C/C_o, versus normalized distance, $d/d_{\max\ water}$ functions for the three replicate transient unsaturated flow columns are shown in Figure 3a−c. Results are plotted on a semilog scale so the differences between θ/θ_s and C/C_o can be readily seen. The C/C_o data were also examined on a linear scale (plots not shown), and it was clear that the distribution of viruses within the column could be reasonably approximated by an exponential decay function.

The θ/θ_s values ranged from 6.68×10^{-1} to 7.72×10^{-1} in the transmission zone adjacent to the inlet and between 1.94×10^{-3} and 3.89×10^{-3} immediately preceding the wetting front. The virus front consistently lagged behind the wetting front. The two dashed vertical lines in Figure 3a–c indicate the centroids of the θ/θ_s, and C/C_o, functions. The centroids divide the area under each curve into two equal parts, although this is not immediately apparent because of the semilog scale. The centroids' λ values are labeled.

Viruses did not travel farther than $d/d_{\max\ water} \approx 0.35$ in any of the unsaturated transient flow column experiments (Figure 3a−c). Most of the viruses were greatly retarded in the first few mm's of the columns. Relative virus concentrations in the first two segments were much greater than unity for replicates 2 and 3 (panels b and c in Figure 3). Replicate 1 was the first column to be run, and it is possible that the lower C/C_o values at the influent end (Figure 3a) were partly related to initial inexperience with the segmentation and/or virus assay procedures.

Steady-State Saturated Flow Experiments. Relative saturation and relative virus concentration expressed as functions of $d/d_{\max\ water}$ for the three replicate steady-state saturated flow columns are graphed in Figure 3d−f. Again, the results are plotted on a semilog scale and the centroid of each curve is indicated. In this case, $\theta/\theta_s = 1$ for all of the segments because the columns were fully saturated. Linear plots of the C/C_o data (not shown) suggested that virus transport during steady-state saturated flow also follows an exponential decay function.

When graphed in terms of normalized distance, the C/C_o profiles for the steady-state saturated flow experiments (Figure 3d−f) were virtually identical to those observed in the transient unsaturated flow experiments (Figure 3a−c). Most of the viruses were again greatly retarded in the first few millimeters of the columns. The C/C_o values within this zone were consistently greater than unity (Figure 3d−f). Viruses never traveled beyond $d/d_{\max\ water} = 0.4$ in the steady-state saturated flow experiments.

Batch Experiments. An adsorption isotherm was constructed for virus partitioning between the solid and liquid phases in the presence of PBS. The partitioning of ϕX174 in PBS was nonlinear, so the data were fitted to a Langmuir isotherm (*39*) using nonlinear regression analysis in the SAS software package:

$$C_s = \frac{BK_L C_w}{1 + K_L C_w} \tag{4}$$

where B is the maximum concentration of sorbed viruses and K_L is a constant related to the binding energy. The resulting parameter estimates ranged from 2.25×10^7 to 6.61×10^7 pfu g^{-1} and from 1.95×10^{-5} to 2.82×10^{-5} mL g^{-1} for B and K_L, respectively. The narrow ranges of variation observed in the parameter estimates indicate the batch experiments were quite reproducible.

Discussion

Mass recovery of viruses ranged from 12 to 61% for the transient unsaturated flow columns and from 19 to 57% for the steady-state saturated flow columns (Table 1). The fact that mass recoveries were similar for both sets of experiments suggests a similar inactivation mechanism. Because air was absent in the steady-state saturated flow experiments, these results point to inactivation or irreversible sorption on the solid phase, which was an untreated natural sample in these experiments. The recoveries in Table 1 are lower than those reported by Chu et al. (*9*) for steady-state transport of ϕX174 in four different sandy materials under unsaturated (36–60%) and saturated (60–166%) flow conditions. In our experiments, recovery was evaluated by washing viruses from each column section into a 15 mL centrifuge tube with BEX solution and then summing the results for all of the sections. In contrast, previous studies (*9, 10, 31*) have evaluated recovery by flushing the entire column with several pore volumes of BEX to desorb viruses. Reduced exposure of viruses to BEX in our study may account for the lower recoveries. Some gravity drainage of PBS solution (and concomitant loss of viruses) during sectioning and sampling of the columns may also partially explain the lower recoveries.

Viruses were constantly introduced into the columns in both types of flow experiment. This explains the high C values near the influent ends of all of the columns. Viruses continued to fill available sorption sites on the Memphis aquifer sand near the influent end, so that as the experiment progressed, the C of viruses within those segments nearest to the column inlet increased beyond C_o. This is to be expected from eq 1. Substituting eq 4 into eq 1, inserting the estimated values of B and K_L and setting $C_w = C_o$ and $\theta = \theta_s$ yielded estimates of C at the influent end of the steady-state saturated flow experiments of between 55 and 65, as compared to measured values for the first segment of between 2.2 and 8.7. The discrepancy is probably related to the poor prediction of retardation by batch experiments (*15*), coupled with the fact

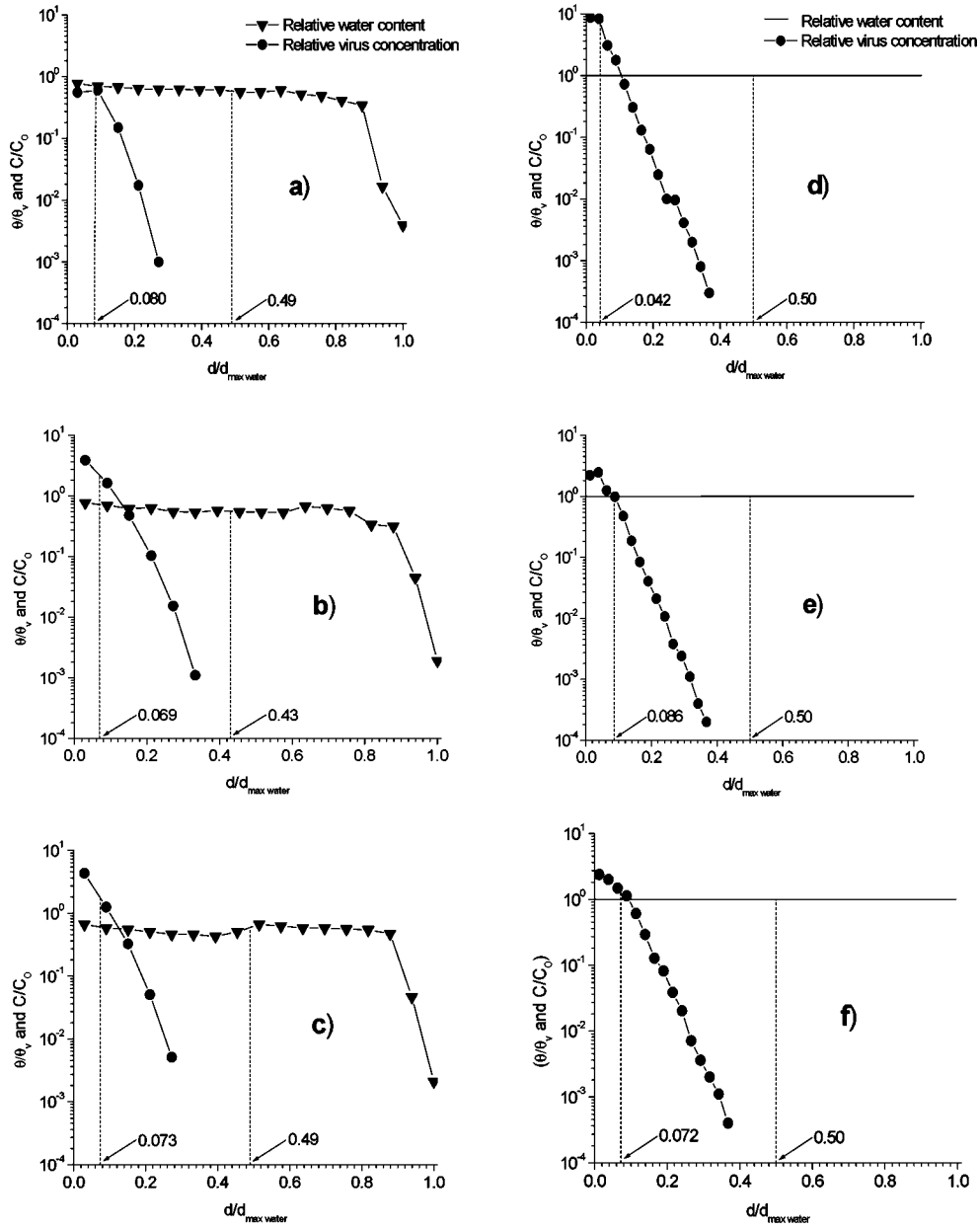

FIGURE 3. Semilog plots of relative water content and relative virus concentration versus relative distance under (a−c) transient unsaturated flow conditions and (d−f) steady-state saturated flow conditions in Memphis aquifer sand. Vertical dashed lines indicate the centroids of the relative water content and virus concentration functions.

that the predictions are for a planar surface at $x = 0$ and not for a column segment of finite length.

Equation 3 was used to compute retardation coefficients, R, based on the ratio of the centroids of the θ/θ_s and C/C_o, functions for both sets of experiments. The results are summarized in Table 1. The average R values for the two flow systems both indicate that significant retardation occurred during transport. The low coefficients of variation indicate that the results were reasonably reproducible from one column to another. The range of steady-state saturated flow R values spans the range of transient unsaturated flow R values for the three replications (Table 1). A two-tailed t test indicated no significant difference between the virus R values during transient unsaturated flow as compared to steady-state saturated flow at $P < 0.05$. This may be attributable to the reduced occurrence of AW/AWS interfaces as the wetting front moves through the sand during transient unsaturated flow. Relative water contents in the wetted zone were close to unity in these experiments (Figure 3a−c). Apparently, any effects of the time varying flow rate, as compared to the time constant flow rate, were negligible in this case.

Retardation coefficients have been reported in several previous virus transport studies (e.g., *40, 41*). To the best of our knowledge, however, the R values in Table 1 are the first for virus transport during transient unsaturated flow. Previous work has compared virus transport under steady-state unsaturated and saturated flow conditions. Viruses typically have lower R values, as evidenced by increased breakthrough, under steady-state saturated flow as compared to steady-state unsaturated flow (*15, 16*). Increased virus sorption/inactivation during steady-state unsaturated flow appears to be due to the presence of AW/AWS interfaces (*9–11*). The similar R values between the two flow regimes used in this study indicate that transient unsaturated flow can produce virus transport similar to steady-state saturated flow. We attribute this result to the similar saturation profiles (Figure

3), which minimized the occurrence of AW/AWS interfaces in both sets of experiments.

Because virus partitioning in the batch experiments was nonlinear, the retardation coefficient will depend upon C_w according to (*39*)

$$R = 1 + \frac{\rho_b B K_L}{\theta(1 + K_L C_w)^2} \quad (5)$$

An effective R value for the batch experiments was calculated for comparison with the steady-state saturated flow experiments by setting C_w in eq 5 equal to the virus concentration in the pore water at λ_v, i.e., $C_w(\lambda_v)$. Estimates of $C_w(\lambda_v)$ were obtained by inserting (eq 4) along with the measured value of C at λ_v and the best estimates of B and K_L into eq 1 and solving the resulting expression for C_w.

On the basis of the $C_w(\lambda_v)$ values for the steady-state saturated flow columns, a mean effective R value of 5096 (CV = 24.1%) was computed for the batch experiments. Again, the low coefficient of variation indicates good reproducibility. The effective batch R value predicts much greater virus retardation at the modal virus concentrations encountered than was actually observed in either of the flow experiments. Powelson and Gerba (*15*) reported R values for three viruses based on batch data that were an order of magnitude higher than those determined from saturated steady-state flow breakthrough curves for the same viruses. These authors suggest that batch R values may not be very useful for modeling virus transport in flowing systems. The large differences between the flow and batch R values observed in our experiments support this assertion.

Our results are for infiltration of a wetting front into air-dry sand. In the field, a range of materials with varying degrees of initial saturation will be encountered. Since virus transport depends greatly on soil properties, similar experiments conducted using different porous media would be useful. Because of the similarity between the retardation factors for transient unsaturated flow and steady-state saturated flow, however, we do not expect any significant dependency of R on initial water content for any given material. Increasing the initial water content of the column would cause a decrease in flow due to the reduction in the capillary driving force. Thus, it would take longer to perform the experiments and there would be a narrower range of water contents over which to evaluate the centroids, but the results should be similar when expressed in terms of relative flow and transport distances.

The ionic strength of the infiltrating solutions employed (0.163 M) was somewhat elevated compared that of most potable groundwater. Thus, the electrical double layer associated with the small amount of fines present was probably compressed, facilitating enhanced attachment of viruses relative to field conditions. At the experimental pH of 7.5, ϕX174 has a relatively weak negative charge because of its pH_{IEP} of 6.6 (*9*). Therefore, one would expect less repulsion of the virus from negatively charged particle surfaces as compared to more negatively charged viruses such as MS2. The presence of metal oxides can overwhelm this effect. On the basis of the Fe content of 8.7 mg kg^{-1}, we assumed that metal oxides were relatively low in the Memphis aquifer sand, although preferential surface coverage of grains remains a possibility. There was a significant amount of calcium present, which in some studies has been shown to increase inactivation and sorption of viruses (*42–44*). Calcium ions could have acted as electrostatic bridges between viruses and negatively charged particles, thereby contributing to the strong sorption observed in our experiments. Both types of experiments (saturated and unsaturated) used the same sand and input solutions, so even though there is some uncertainty regarding the exact nature of the retention mechanisms involved, the results still provide a valid comparison of transport under different flow conditions.

This study described the extent and rate of bacteriophage ϕX174 transport under transient unsaturated flow and steady-state saturated flow conditions in Memphis aquifer sand columns. A new approach to calculating virus retardation was employed that permits direct comparison between virus R values for the two different flow regimes studied. This approach could also be applied to quantify virus retardation in steady-state unsaturated flow experiments. Convenient methods for determining R under transient flow conditions, such as the one reported here, may prove useful for future research on virus transport.

Our results support the hypothesis that virus retardation during transient unsaturated flow is similar to virus retardation during steady-state saturated flow. This is likely due to a reduction in the number of AW/AWS interfaces under both conditions as compared to steady-state unsaturated flow in which air–water menisci are distributed throughout the entire porous medium. This finding has significant implications for land applications of treated and untreated sewage effluent, where transient unsaturated flow conditions predominate. The fact that virus R values for transient unsaturated and steady-state saturated flows were similar argues against the notion that the vadose zone provides an additional level of protection for groundwater resources, over and above that provided by retardation occurring below the water table.

Acknowledgments

This research was funded in part by the Center for Environmental Biotechnology at the University of Tennessee, the Geological Society of America, and Sigma Xi Scientific Research Society. The Memphis aquifer sand samples were supplied by Dr. Randy Gentry of the Department of Civil and Environmental Engineering, University of Tennessee. Dr. Jaehoon Lee of the Department of Biosystems Engineering and Soil Science at the University of Tennessee allowed us to use his tension table setup. Julie Higgins of the Department of Microbiology at the University of Tennessee provided guidance and technical expertise concerning virus assay techniques.

Literature Cited

(1) Atlas, R. M. Microbial pollutants in our nation's water; Environmental and public health issues: A national call for action. *OECD Workshop Molecular Methods for Safe Drinking Water*; American Society of Microbiology: Interlaken, Switzerland, 1998.
(2) Craun, G. F. *Waterborn Diseases in the United States*; CRC Press: Boca Raton, FL, 1986.
(3) Macler, B. A.; Merkle, J. C. Current knowledge on groundwater microbial pathogens and their control. *Hydrogeol. J.* **2000**, *8*.
(4) Woessner, W. W.; Ball, P. N.; DeBorde, D. C.; Troy, T. L. Viral transport in a sand and gravel aquifer under field pumping conditions. *Ground Water* **2001**, *39*, 886–894.
(5) Rosen, B. H. *Waterborne Pathogens in Agricultural Watersheds*; NRAES: Ithaca, NY, 2001.
(6) Jin, Y.; Flury, M. Fate and transport of viruses in porous media. *Adv. Agron.* **2002**, *77*, 39–102.
(7) Karkare, M. V.; Fort, T. Determination of the air-water interfacial area in wet "unsaturated" porous media. *Langmuir* **1996**, *12*, 20412044..
(8) Cary, J. W. Estimating the surface area of fluid phase interfaces in porous media. *J. Contam. Hydrol.* **1994**, *15*, 243–248.
(9) Chu, Y.; Jin, Y.; Baumann, T.; Yates, M. V. Effect of soil properties on saturated and unsaturated virus transport through columns. *J. Environ. Qual.* **2003**, *32*, 2017–2025.
(10) Chu, Y.; Jin, Y.; Flury, M.; Yates, M. V. Mechanisms of virus removal during transport in unsaturated porous media. *Water Resour. Res.* **2001**, *37*, 253–263.
(11) Torkzaban, S.; Hassanizadeh, S. M.; Schijven, J. F.; de bruin, H. A. M.; de Roda Husman, A. M. Virus transport in saturated and unsaturated sand columns. *Vadose Zone J.* **2006**, *5*, 877–885.

(12) Jin, Y.; Chu, Y.; Li, Y. Virus removal and transport in saturated and unsaturated sand columns. *J. Contam. Hydrol.* **2000**, *43*, 111–128.
(13) Lance, J. C.; Gerba, C. P. Virus movement in soil during saturated and unsaturated flow. *Appl. Environ. Microbiol.* **1984**, *47*, 335–341.
(14) Van Cuyk, S.; Siegrist, R. L. Virus removal within a soil infiltration zone as affected by effluent composition, application rate, and soil type. *Water Res.* **2007**, *41*, 699–709.
(15) Powelson, D. K.; Gerba, C. P. Virus removal from sewage effluents during saturated and unsaturated flow through soil columns. *Water Res.* **1994**, *28*, 2175–2181.
(16) Powelson, D. K.; Simpson, J. R.; Gerba, C. P. Virus transport and survival in saturated and unsaturated flow through soil columns. *J. Environ. Qual.* **1990**, *19*, 396–401.
(17) Van Cuyk, S.; Siegrist, R. L.; Lowe, K.; Harvey, R. W. Evaluating microbial purification during soil treatment of wastewater with multicomponent tracer and surrogate tests. *J. Environ. Qual.* **2004**, *33*, 366–329.
(18) Flint, A. L.; Flint, L. E. Particle density. *Methods of Soil Analysis: Part 4—Physical Methods*; Soil Science Society of America: Madison, WI, 2002; pp 229–240.
(19) Kutílek, M.; Nielsen D. R. *Soil Hydrology*; Catena Verlag: Cremlingen-Destedt, Germany, 1994.
(20) Reynolds, W. D.; Elrick, D. E.; Youngs, E. G.; Amoozegar, A.; Booltink, H. W. G. et al. Saturated and field-saturated water flow parameters. *Methods of Soil Analysis: Part 4—Physical Methods*; Soil Science Society of America: Madison, WI, 2002; pp 797–878.
(21) Mehlich, A. *Determination of P, Ca, Mg, K, Na, and NH_4*; North Carolina Soil Test Division: Raleigh, NC, 1953.
(22) Walkley, A.; Black, I. A. An examination of Degtjareff method for determining soil organic matter and a proposed modification of the chromic acid titration method. *Soil Sci.* **1934**, *37*, 29–37.
(23) Thomas, G. W. Soil pH and Soil Acidity. *Methods of Soil Analysis: Part 3—Chemical Methods*; Soil Science Society of America: Madison, WI, 1996; pp 475–490.
(24) Newby, D. T.; Pepper, I. L.; Maier, R. M. Microbial Transport. *Environmental Microbiology*; Academic Press: New York, 2000; pp 147–175.
(25) Redman, J. A.; Grant, S. B.; Olson, T. M.; Hardy, M. E.; Estes, M. K. Filtration of recombinant Norwalk virus particles and bacteriophage MS2 in quartz sand: Importance of electrostatic interactions. *Environ. Sci. Technol.* **1997**, *31*, 3378–3383.
(26) Ackerman, H. W.; Dubow, M. S. *Viruses of Prokaryotes*; CRC Press: Boca Raton, FL, 1987.
(27) Adams, M. H. *Bacteriophage*; Interscience: New York, 1959.
(28) Snyder, L. R.; Kirkland, J. J. *Introduction to Modern Liquid Chromatography*; Wiley: New York, 1979.
(29) Chu, Y.; Jin, Y.; Yates, M. V. Virus transport through saturated sand columns as affected by different buffer solutions. *J. Environ. Qual.* **2000**, *29*, 1103–1110.
(30) Jin, Y.; Yates, M. V.; Thompson, S. S.; Jury, W. A. Sorption of Viruses during Flow through Saturated Sand Columns. *Environ. Sci. Technol.* **1997**, *31*, 548–555.
(31) Zhuang, J.; Jin, Y. Virus retention and transport through Al-oxide coated sand columns: Effects of ionic strength and composition. *J. Contam. Hydrol.* **2003**, *60*, 193–209.
(32) Smiles, D. E.; Philip, J. R.; Knight, J. H.; Elrick, D. E. Hydrodynamic dispersion during absorption of water by soil. *Soil Sci. Soc. Am. J.* **1978**, *42*, 229–234.
(33) Clothier, B. E.; Sauer, T. J.; Green, S. R. The movement of ammonium nitrate into unsaturated soil during unsteady absorption. *Soil Sci. Soc. Am. J.* **1988**, *52*, 340–345.
(34) Duwing, C.; Becquer, T; Charlet, L.; Clothier, B. E. Estimation of nitrate retention in a Ferralsol by a transient-flow method. *Eur. J. Soil Sci.* **2003**, *54*, 505–515.
(35) Katou, H.; Uchimura, K.; Clothier, B. E. An unsaturated flow method for determining solute adsorption by variable-charge soils. *Soil Sci. Soc. Am. J.* **2001**, *65*, 283–290.
(36) Ahmad, R.; Katou, H.; Kookana, R. S. Measuring sorption of hydrophilic organic compounds in soils by an unsaturated transient flow method. *J. Environ. Qual.* **2005**, *34*, 1045–1054.
(37) Bartoli, F.; Boivin, A.; Schiavon, M. Water and herbicide transient flow transport in field-dried topsoils during controlled infiltration. II. Herbicide capillary and gravity-driven transient flows. *Geoderma* **2006**, *136*, 494–503.
(38) Ochsner, T. E.; Stephens, B. M.; Koskinen, W. C.; Kookana, R. S. Sorption of a hydrophilic pesticide: Effects of soil water content. *Soil Sci. Soc. Am. J.* **2006**, *70*, 1991–1997.
(39) Papiernik, S. K.; Yates, S. R. Processes governing transport of organic solutes. *Methods of Soil Analysis: Part 4—Physical Methods*; Soil Science Society of America: Madison, WI, 2002; pp 1451–1479.
(40) Bales, R. C.; Hinkle, S. R.; Kroeger, T. W.; Stocking, K.; Gerba, C. P. Bacteriophage adsorption during transport through porous media: Chemical perturbation and reversibility. *Environ. Sci. Technol.* **1991**, *25*, 2088–2095.
(41) Bales, R. C.; Gerba, C. P.; Grondin, G. H.; Jensen, S. L. Bacteriophage transport in sandy soil and fractured tuff. *Appl. Environ. Microbiol.* **1989**, *55*, 2061–2067.
(42) Burge, W. D.; Enkiri, N. K. Adsorption kinetics of bacteriophage φX174 on soil. *J. Environ. Qual.* **1978**, *7*, 536–541.
(43) Goyal, S.; Gerba, C. P. Comparative adsorption of human enteroviruses, simian rotavirus and selected bacteriophages to soils. *Appl. Environ. Microbiol.* **1979v**, *38*, 241–247.
(44) Yates, M. V.; Gerba, C. P.; Kelly, L. M. Virus persistence in groundwater. *Appl. Environ. Microbiol.* **1985**, *49*, 778–781.

ES071213S